
BAYESIAN PARAMETERIZED QUANTUM CIRCUIT OPTIMIZATION (BPQCO): A TASK AND HARDWARE-DEPENDENT APPROACH

A PREPRINT

✉ **Alexander Benítez-Buenache**

Department of Artificial Intelligence and Big Data
GMV

Isaac Newton, 11, Tres Cantos, 28760, Madrid, Spain
abenitez@gmv.com

✉ **Queralt Portell-Montserrat**

Department of Artificial Intelligence and Big Data
GMV

Isaac Newton, 11, Tres Cantos, 28760, Madrid, Spain
qqpm@gmv.com

April 18, 2024

ABSTRACT

Variational quantum algorithms (VQA) have emerged as a promising quantum alternative for solving optimization and machine learning problems using parameterized quantum circuits (PQCs). The design of these circuits influences the ability of the algorithm to efficiently explore the solution space and converge to more optimal solutions. Choosing an appropriate circuit topology, gate set, and parameterization scheme is determinant to achieve good performance. In addition, it is not only problem-dependent, but the quantum hardware used also has a significant impact on the results. Therefore, we present BPQCO, a Bayesian Optimization-based strategy to search for optimal PQCs adapted to the problem to be solved and to the characteristics and limitations of the chosen quantum hardware. To this end, we experimentally demonstrate the influence of the circuit design on the performance obtained for two classification problems (a synthetic dataset and the well-known Iris dataset), focusing on the design of the circuit ansatz. In addition, we study the degradation of the obtained circuits in the presence of noise when simulating real quantum computers. To mitigate the effect of noise, two alternative optimization strategies based on the characteristics of the quantum system are proposed. The results obtained confirm the relevance of the presented approach and allow its adoption in further work based on the use of PQCs.

Keywords Parameterized Quantum Circuits · Ansatz design · Bayesian Optimization · Noisy hardware

1 Introduction

The last few years can be regarded as the ultimate outcome of a journey that has been underway for decades towards the creation of impressive Artificial Intelligence (AI) systems. This progress is primarily attributed to the evolution of Machine Learning (ML) techniques [Bishop and Bishop, 2023]: Neural networks (increasingly complex), attention mechanism, or the rise of generative AI, to cite a few examples. The evolution of hardware has played a significant role in facilitating the execution of training models, particularly through the use of GPUs and distributed computing. Consequently, large data sets can now be processed seamlessly. This ongoing evolution is leading to an increasing number of applications and improved performance.

However, alongside the aforementioned development, a new area of research has arisen in the scientific community called Quantum Machine Learning (QML) [Biamonte et al., 2017] [Maria Schuld and Petruccione, 2015], and it is becoming increasingly relevant. This new approach seeks to incorporate the principles of Quantum Computing (QC) into Machine Learning solutions. Thus, the aim is to incorporate the Physics properties of quantum states, such as superposition, interference or entanglement when carrying out the necessary calculations and operations. The main goal of this new paradigm is to achieve better solutions in terms of computational speed, better performance (the so-called quantum supremacy or quantum advantage) or even improvements in terms of energy consumption. QC represents a fundamental change in the handling of information. This computing approach sets the qubit (or quantum bit) as the

basic unit of information. The primary contrast is that while a bit can represent either state 0 or state 1, a qubit can coexist simultaneously in a linear combination of states 0 and 1, thanks to the property of superposition of quantum states. To be clearer, if $|0\rangle$ and $|1\rangle$ are the two possible levels, a general quantum state $|\psi\rangle$ of this system is represented by $|\psi\rangle = \alpha|0\rangle + \beta|1\rangle$, with $\alpha, \beta \in \mathbb{C}$ and $|\alpha|^2 + |\beta|^2 = 1$.

Furthermore, qubits can be entangled. This is a quantum physics phenomenon where two particles are closely correlated so that there is a co-dependence between them in describing each other’s quantum state, even when they are separated. It is important to note that this property will be of great importance when dealing with correlated data.

Quantum circuits are used to interact with quantum states. The circuits consist of a sequence of quantum gates, each of which acts as a unitary (*i.e.*, reversible) operator. The primary functions of quantum gates include producing superposition states, phase modification, and generating entanglement. Additionally, the measurement of qubits in these circuits is noteworthy as it involves the collapse of a qubit into a quantum state. For instance, a qubit in the $|+\rangle$ state has an equal chance of obtaining 0 or 1 after measurement. However, the qubit will collapse into the state ($|0\rangle$ or $|1\rangle$) that has been measured. Hence, the measurement affects the quantum state of the system. By exploiting the physical properties described above, the combination of these gates allows the design of quantum algorithms, of which Shor’s and Grover’s algorithms are well-known examples. Throughout this paper it is assumed the knowledge of the different operations by means of quantum gates. Nevertheless, if the reader wants to become familiar with it, it is recommended to read [Nielsen and Chuang, 2010].

Despite the benefits of quantum computing that have been presented above, there are currently several limitations to this technology. In fact, this current period is known as the Noisy Intermediate-Scale Quantum (NISQ) era [Preskill, 2018], relative to the actual capabilities of quantum hardware. Typically, the low number of qubits has been the main limitation of quantum computers, which restricts the complexity and the amount of information that can be processed. For each quantum computer with N qubits, there are 2^N quantum states within it. As a result, the number of possible quantum states increases exponentially with the number of qubits. Although this remains a limitation, it is worth noting the recent progress in the number of qubits available, which now exceeds a few hundred. Nevertheless, the main limitation of quantum systems in this NISQ era is the vulnerability of qubits to factors such as decoherence or quantum noise. This vulnerability results in computational errors due to the intrinsic hardware characteristics and external factors such as electromagnetic fields or thermal fluctuations. Additionally, each quantum computer has a different coupling map (scheme of possible connections between qubits) and, with few exceptions, not all qubits are fully connected to each other. Even the allowed gates may vary for each system. Thus, the circuits are transpiled. The goal of the transpiler is to adapt the circuit to be executed on a particular quantum computer. This process usually involves a drastic change in the circuit with respect to the ideal design, resulting in more complex and deeper (increasing gate layers) circuits. Obviously, the greater the depth, the greater the vulnerability to noise effects. For all these reasons, the importance of designing a suitable circuit is worth noting.

Nonetheless, the above limitations present a valuable opportunity to further research the field from both a hardware and algorithmic perspective. Undoubtedly, this parallel progress of algorithms and hardware has a strong analogy with the process carried out by classical ML, mentioned in the first lines of this section. In fact, the development of quantum algorithms, particularly QML algorithms, has been exceptional in recent years [Zaman et al., 2023][Combarro et al., 2023]. As might be expected, most existing QML algorithms have emerged as adaptations of their classical counterparts. Good examples are Quantum Support Vector Machine (QSVM) [Rebentrost et al., 2014], Quantum Neural Networks [Henderson et al., 2020], Quantum Convolutional Neural Networks (QCNNs) [Oh et al., 2020], or Quantum Recurrent Neural Networks (QRNNs) [Takaki et al., 2021], to name a few. During the NISQ era, the primary approach is to evolve algorithms beyond the hardware restrictions. This has facilitated the progression of QML architectures design for solving small problems. However, the goal is to be prepared for hardware advances to tackle real-world problems, such as datasets with large amounts of data with multiple variables. In addition to this purely quantum approach, there are hybrid solutions [Sim et al., 2019] [Endo et al., 2021]. This approach aims to solve concrete tasks of a classical ML architecture in a quantum manner.

Within this brief compendium of techniques, Variational Quantum Algorithms (VQAs) stand out. This family of algorithms is based on the use of Parameterized Quantum Circuits (PQCs) [Benedetti et al., 2019]. As the name suggests, these circuits are designed to solve specific problems by optimizing a series of parameters, which commonly refers to the angle of a rotation gate. There are two main types of algorithms within the VQAs: Variational Quantum Eigensolvers (VQEs) and Variational Quantum Classifiers (VQCs). VQE is a quantum algorithm used to find approximations to the lowest energy states (eigenvalues) and corresponding eigenvectors of a Hamiltonian associated with a quantum system. It is typically used in optimization problems, but also in other tasks such as quantum chemistry and simulation. Similarly, VQCs use PQCs to implement classification models. These parameterized circuits are iteratively optimized using classical methods to minimize a loss function that measures the discrepancy between model predictions and the true labels of the training data. This type of circuit has the advantage of being easily integrated in hybrid architectures,

i.e., architectures that combine quantum and classical layers in their structure. Thus, certain classical parameters, such as neural network weights, are replaced by rotation angles of the PQC. Various papers in the literature provide examples of this [Sakhnenko et al., 2022][Chen et al., 2022][Maheshwari et al., 2022] [Sagingalieva et al., 2023] [Chen et al., 2024]. However, these circuits are problem-specific, meaning that the circuit’s architecture (including the number of qubits, entanglement, gates, etc.) will depend on the problem that needs to be solved [Sim et al., 2019]. While circuit templates [Nakata et al., 2017] [Hubregtsen et al., 2021] may be useful for certain tasks, it is important to note that there is no universal architecture that solves all problems. As a result, designing these circuits presents a significant new challenge, which is addressed in this paper. Ideally, designing the optimal quantum circuit would require time and knowledge of both the problem and quantum circuit design. However, this is impractical. Therefore, various search criteria have been studied, including the use of brute force [Raubitsek and Mallinger, 2023], genetic algorithms [Altares-López et al., 2024], Bayesian optimization [Pirhooshyaran and Terlaky, 2021], reinforcement learning [Pirhooshyaran and Terlaky, 2021], or based on neural networks [Du et al., 2022].

Approaches such as those mentioned above can help build effective circuits for specific problems, resulting in good performance. However, most approaches focus on designing ideal solutions without considering the current limitations of quantum hardware. As a result, when implementing these circuits on real hardware, their performance significantly degrades. Recent works [Buonaiuto et al., 2024] has already explored possible alternatives to take into account the coupling map in specific hardware. In this context, we present a PQC design methodology, in which we highlight the following aspects:

- Proposal of a complete and detailed process of PQC design, including notation to formulate the different variables to be explored during the search.
- Experimental tests that prove the effect of the circuit design on the results obtained.
- Demonstration of the vulnerability to noise of previously created designs in ideal environments.
- Presentation of two design alternatives that consider the characteristics and limitations of real quantum hardware.

The rest of the paper is structured as follows. Section 2 presents and details important criteria for designing PQCs. Section 3 introduces BPQCO (Bayesian Parameterized Quantum Circuit Optimization), the proposal for circuit design using Bayesian Optimization, being evaluated with experimental examples in Section 4. Section 5 evaluates the possible degradation in noisy environments of the obtained circuits and proposes an alternative to include the limitations of real hardware in the design process. Finally, Section 6 presents the conclusions drawn from the work and future lines to be explored.

2 On the design of Parameterized Quantum Circuits

Although there is no single structure of PQCs, several authors [Benedetti et al., 2019] [Du et al., 2022][Maheshwari et al., 2022] point to the existence of two main blocks within the circuit: the feature map for data encoding and the ansatz. The first refers to the encoding of information in the circuit. That is, any d -dimensional data is transformed through a series of operations/gates to encode it as a quantum state. On the other hand, the ansatz is the most important part of the circuit, as its parameters are the solution to the problem to be solved. In the design of both blocks there are numerous options and criteria to take into account. In fact, both parts can be repeated or mixed with each other throughout the circuit. This section describes some of the key details of this design process to help the reader understand how it works and how it can be put into practice.

2.1 Feature map

Usually, classical data is represented as quantum states using a quantum feature map. Let \mathcal{X} be the set of the input classical data. Then, a quantum feature map is a function $\phi : \mathcal{X} \rightarrow \mathcal{F}$, where \mathcal{F} is a Hilbert space and the feature vectors are quantum states. Using a unitary transformation $U_\phi(x)$ it transforms $x \rightarrow |\phi(x)\rangle = U_\phi(x)|0\rangle$.

Thus, choosing an appropriate feature map is the first step in building a PQC, as it can affect performance, efficiency, and error susceptibility. The selection of a method for encoding data depends on various factors, such as the type of data (tabular, image, time series, etc.), the number of dimensions, and the number of qubits available on the chosen quantum computer. However, it is important to note that finding an encoder with enough expressive capacity to represent the information in the input data is sufficient. In practice, the most common methods for quantum encoding are basis encoding, amplitude encoding and angle encoding [Schuld and Killoran, 2019] [Weigold et al., 2021]. Also of note is the ZZFeatureMap –used in later sections–, a circuit that encodes each feature of the data in a wire (*i.e.*, the number of qubits required matches the number of features). This quantum circuit implements $U_\phi(x)$ by means of Hadamard

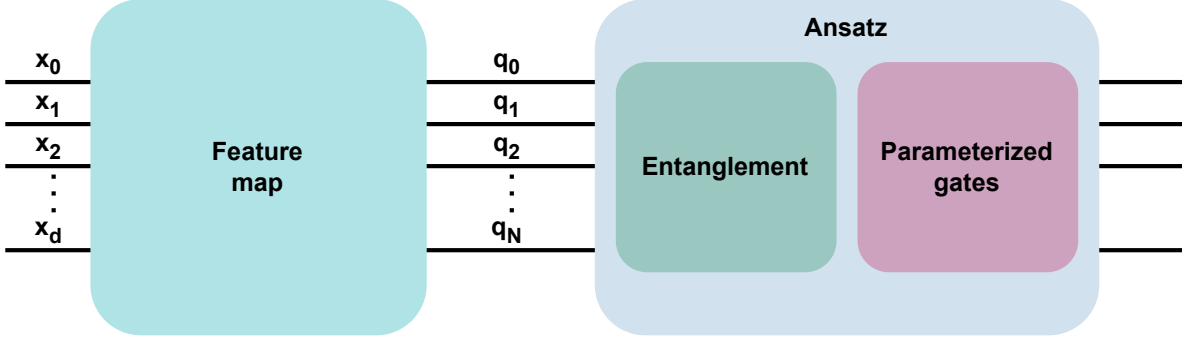


Figure 1: Schematic representation of the structure of an N-qubit PQC.

(H) gates to create superposition, as they transform the $|0\rangle$ state into $1/\sqrt{2}(|0\rangle + |1\rangle)$. In addition, it also contains single-qubit rotations about the Z axis (whose angles depend on the value of the input’s features) and CNOT gates.

Finally, it is worth mentioning the possibility of using the data re-uploading technique, which has been shown to improve the performance of a universal quantum classifier [Pérez-Salinas et al., 2020]. This technique is based on repeating the encoding block along the circuit.

2.2 Ansatz

After designing the encoder to inject the input data into the quantum circuit, it is time to design the ansatz. The ansatz is key in PQC as it provides the solution to the problem. The circuit’s architecture is determined by the design of its components, such as the number of qubits, the level of entanglement, the depth, or the gates that are included. This has a major impact on the performance of the solution. However, their choice is not straightforward and is strongly problem-dependent. Therefore, this paper aims to help in the design of the ansatz architecture, as presented in the next section.

Within the ansatz there are two main components: The gates that introduce the entanglement and the parameterized gates whose values are adjusted during training. Both blocks will be described in detail below. However, it is worth noting that they are not necessarily two sequential and distinguishable blocks, but two components to be considered.

As mentioned above, one of the main properties of quantum states is entanglement, which is the capacity of a quantum state in a qubit to influence the state of another qubit. There are several ways of creating entanglement between qubits, but the most common is to include a Hadamard gate followed by a CNOT. CNOT is a two-qubit gate that leaves the control qubit unchanged. If the control qubit is in the state $|1\rangle$ applies a Pauli-X rotation in the target qubit, and if it is in the state $|0\rangle$ leaves the target qubit unchanged. During the design phase of a PQC, layers of different two-qubit gate configurations, such as CNOT, CZ and other parameterized variants, are often added and repeated to produce strongly entangled circuits [Sim et al., 2019].

On the other hand, the ansatz will contain the part of the circuit whose parameters θ will be selected during training as the solution to the problem. Given a training dataset $\mathcal{X} = \{\mathbf{x}^{(n)}, t^{(n)}\}, n = \{1, 2, \dots, N\}$, where \mathbf{x} represents its features and t its labels, the parameterized gates will act as a function \mathcal{F} to reach the quantum state $\langle \hat{\mathcal{B}} \rangle = \mathcal{F}(\mathbf{x}; \theta)$ from the θ parameters. Thus, during circuit training, the aim is to achieve an optimal (or at least good enough) set of parameters

$$\theta^* = \operatorname{argmin}_{\theta} \sum_N c(t, \langle \hat{\mathcal{B}} \rangle), \tag{1}$$

where c represents the subrogated cost (or loss function), a function that quantifies the error of the system output. In other words, the aim is to obtain the parameters that allow the input data to be transformed into a quantum state that allows the different classes of the classification problem to be distinguished.

Within the PQC, these parameters are a series of rotation angles that are applied on the different qubits by means of rotation gates (RX, RY and RZ). The angle $\theta \in \{0, 2\pi\}$ defines the rotation around the quantum state of the qubit in the X, Y and Z axes of the Bloch sphere¹. Figure 2 shows three examples of rotation using each of these gates. In addition,

¹The Bloch sphere is a geometric representation to visualise the states of a qubit. It maps the possible quantum states onto the surface of a unit sphere, where the poles represent the basis states $|0\rangle$ and $|1\rangle$ and the points on the sphere’s surface represent superposition of these states.

these rotations can be controlled by another qubit in the same way as for the CNOT gate. If the control qubit is in the state $|1\rangle$, the corresponding rotation is applied to the target qubit. Whereas if the control qubit is in the state $|0\rangle$, the target qubit remains unchanged. These controlled gates will be referred as CRX_{ij} , CRY_{ij} and CRZ_{ij} , where the indices i and j indicate that the qubit q_i is the control qubit and the qubit q_j is the target qubit.

Once the possible gates for the design have been presented, it is necessary to select the architecture. This is a process similar to the definition of a classical neural network, which requires certain criteria to decide on aspects such as the number of hidden layers, the number of neurons in each layer and other hyperparameters that are not trainable. In this case, the choices are the configuration of the rotation gates for each qubit wire in terms of the number of gates (depth of the circuit), the type of rotation gate (axis of rotation and number of qubits involved in the rotation) and the position of each of them. In fact, the order and position of the gates can have a major impact on the performance of the PQC. This fact motivates the possibility of using search criteria to obtain an optimal (or at least a good enough) circuit, as presented in the following section.

3 BPQCO: A Bayesian Optimization approach for PQC design

As seen in the previous section, there are numerous aspects and criteria for the design of a quantum circuit. Beyond the possibility of carrying out preliminary exploratory studies to analyse the possible effects of incorporating certain gates, the number of possibilities and the need to train the system to see the performance (with the time involved) makes brute force approaches unfeasible. It is therefore necessary to establish other types of strategies to maximize performance for a given problem. This paper proposes BPQCO (Bayesian Parameterized Quantum Circuit Optimization), a Bayesian Optimization based approach to address this need. This option has been explored in some previous works [Pirhooshyaran and Terlaky, 2021], [Koike-Akino et al., 2022] with promising results. However, the aim is to go one step further with more complex architectures and an exhaustive analysis of the behaviour of the solutions obtained (as will be seen in later sections).

To this end, we propose to define each possible gate position as a hyperparameter of the PQC to be designed. Each hyperparameter can take different values depending on the circuit block in which it is included. Then, based on a Bayesian optimization process, the values (gates) that maximise the performance of the circuit are selected. This process is detailed below, including the definition of each hyperparameter to be explored and the proposed search method.

3.1 PQC architecture to be explored

To optimize the circuit architecture, it is necessary to define some design criteria first. This paper follows the scheme presented in Section 2, which consists of a feature map followed by the ansatz, including entanglement and parameterized gates. However, it is also valid to consider alternative options, such as fixing certain components or rearranging the order of elements. Therefore, the objective is to select the optimal circuit $\mathcal{C}^* = (\mathcal{D}, \mathcal{M}, \mathcal{E}, \mathcal{P})$ that maximizes performance, with \mathcal{D} being design parameters (such as the number of qubits or the circuit depth), \mathcal{M} the feature map, \mathcal{E} the entanglement, and \mathcal{P} the parameterized gates.

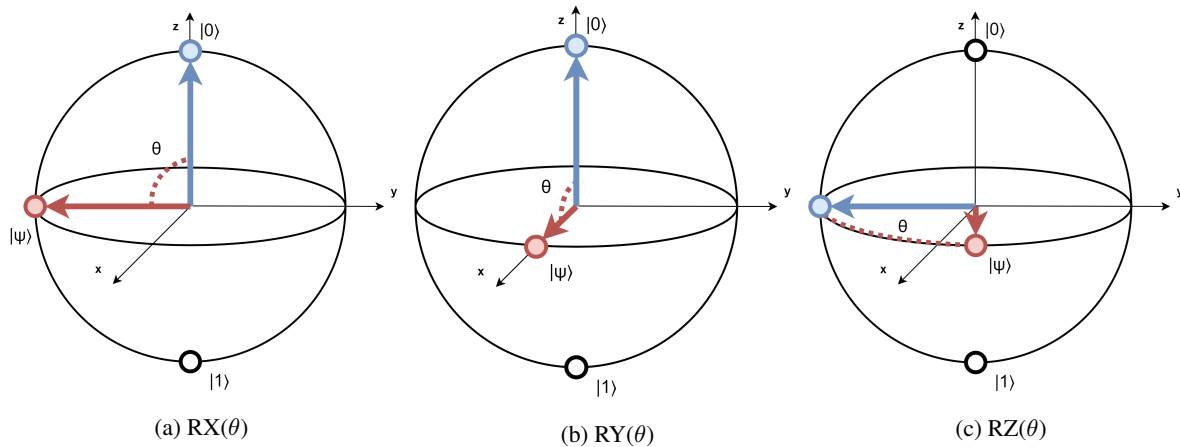


Figure 2: Bloch sphere representation of the quantum state $|\psi\rangle$ change due to rotation θ at gates RX , RY and RZ , respectively. In blue the initial state and in red the state after rotation.

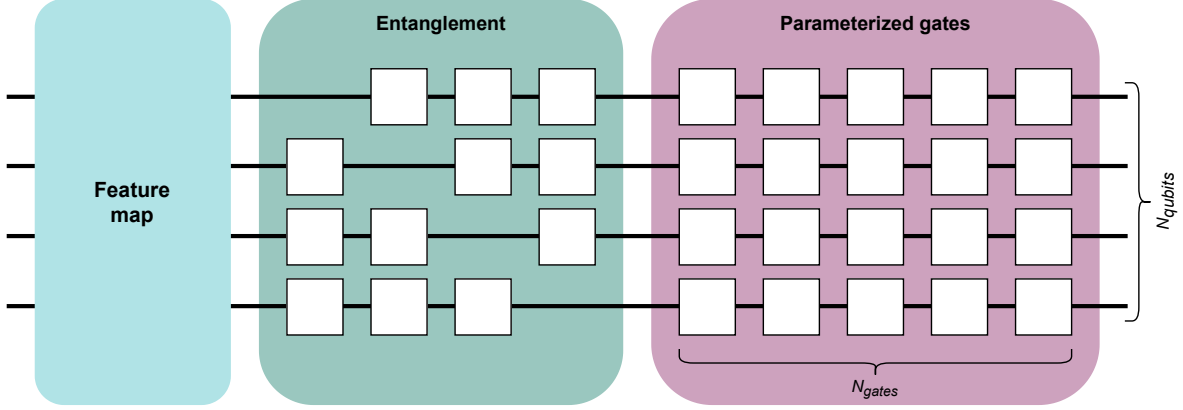


Figure 3: Graphical description of the design elements to be selected during circuit optimization. Each white block represents the position where a gate can be selected.

The circuit optimization process can include the choice of design parameters \mathcal{D} to consider circuits with varying numbers of qubits (N_{qubits}) or depth (N_{gates}) for optimal performance. However, these aspects can be predetermined through exploratory tests based on hardware or resource constraints such as computation time and simulation system memory.

In terms of the feature map, there are several options to consider, including the encoding method and the intrinsic parameters of these methods, such as the angle of rotation. Each option determines a parameter to explore during optimization. However, as previously mentioned, for the encoding it is sufficient to find a method to adapt the information with enough expressiveness. Therefore, it is recommended to establish \mathcal{M} a priori, after conducting some preliminary exploratory tests.

The proposed method for selecting the gates that introduces entanglement between qubits involves using matrix

$$\hat{\mathcal{E}} = \begin{cases} 0, & \forall i = j; i, j = 0, 1, \dots, N_{qubits} - 1 \\ e_{ij} \in \{0, 1\}, & \forall i \neq j; i, j = 0, 1, \dots, N_{qubits} - 1, \end{cases} \quad (2)$$

which consists of $(N_{qubits} \times N_{qubits})$ binary variables. Each variable represents the presence or absence of a CNOT gate between qubits i and j for their entanglement. For obvious reasons, the diagonal is always zero, since it is impossible to create entanglement between a qubit and itself.

On the other hand, the configuration of parameterized gates that form the ansatz solution are modeled by

$$\hat{\mathcal{P}} = p_{ik} \in \{\text{None}, \text{RX}, \text{RY}, \text{RZ}, \text{CRX}_{ij}, \text{CRY}_{ij}, \text{CRZ}_{ij}\} \\ i, j = 0, 1, \dots, N_{qubits} - 1, j \neq i, \\ k = 0, 1, \dots, N_{gates} - 1, \quad (3)$$

a matrix of size $(N_{qubits} \times N_{gates})$ composed of categorical variables. Each variable represents a parameterized gate that will be placed at each position k of the i -qubit. As shown in (3), the available options include one-qubit and two-qubit (controlled) rotation gates, as well as the option of not including any gate (None).

To ensure efficient use of the gates and to avoid increasing the circuit depth unnecessarily, it is recommended to apply post-processing criteria. To this end, we propose to establish two criteria: 1) Remove repeated consecutive gates only if they are simple rotations or if there is no gate in the qubit with which it is entangled; 2) Eliminate RZ gates in the last position since, being measured in z, they only affect the global phase.

Figure 3 illustrates the proposed circuit structure. However, as mentioned earlier, there are numerous design possibilities. For instance, in the figure, the entanglement and parameterized gates appear as independent components. However, an alternative approach would be to combine them into a single block where either CNOT gates or rotation gates are selected for each position. Therefore, it is important to note that regardless of the initial design criteria, the use of a circuit optimization method is essential, as explained below.

3.2 BPQCO by means of TPE algorithm

After defining the options for building the PQC, it is necessary to establish an optimization strategy. For this purpose, we propose BPQCO, a Bayesian optimization process based on the Tree-structured Parzen Estimator (TPE) algorithm

[Bergstra et al., 2011]. The TPE algorithm is commonly used in ML for hyperparameter optimization. To accomplish this, an objective function must be chosen to evaluate performance and then minimized or maximized accordingly. In this case, the hyperparameter to be evaluated are those defined in the previous section (\mathcal{D} , \mathcal{M} , \mathcal{E} , \mathcal{P}). These hyperparameters are defined as binary and categorical variables according to (2) and (3), respectively. The usual strategy for optimizing an objective function assumes that the objective function exists in a continuous domain. Therefore, the algorithm rounds the proposed continuous points to the nearest discrete points. During the optimization process, a guided and efficient search is conducted towards promising regions of the hyperparameter space using a probabilistic model of both evaluated and non-evaluated parameters. Thus, several combinations of hyperparameters are evaluated during the search by means of trails. The benefit of this approach is that, after a limited number of trials, a good value for the objective function is achieved.

To do this, the BPQCO process selects circuits (trials) that are trained and tested in a validation subset. Each of these circuits obtains a metric in this validation subset, which will be the objective function of the Bayesian optimization process. After the guided search, the circuit with the best metric is selected.

4 Experimental examples

This section provides examples of how the proposed BPQCO methodology works. For the tests, we have chosen two classification problems (binary and multiclass). Therefore, the selected algorithm for the task is a VQC. Thus, the main goal is to find the ansatz that gives the best possible performance for each classification problem. That is, not to use a pre-defined ansatz, but to adapt it to the specific problem to be solved.

4.1 Datasets

A synthetic dataset and a real-world problem have been used for testing. Both are described below:

- **Synthetic dataset (binary classification):** This synthetic dataset has been generated by creating clusters of $4-d$ points normally distributed about vertices of a bidimensional hypercube with sides of length 0.8. In this case, an equal number of clusters is assigned to each class. The number of generated samples is 1000 with a class imbalance ratio of 65 : 35 and a class separation of 0.4. Figure 4 shows the distribution of both classes.
- **Iris dataset (multiclass classification):** The Iris dataset [Fisher, 1988] contains 150 instances described by four continuous features. The objective is to classify the three types of Iris plant: Setosa, Versicolour, and Virginica. It is a well-known dataset typically used in ML research. It is an easy problem with high

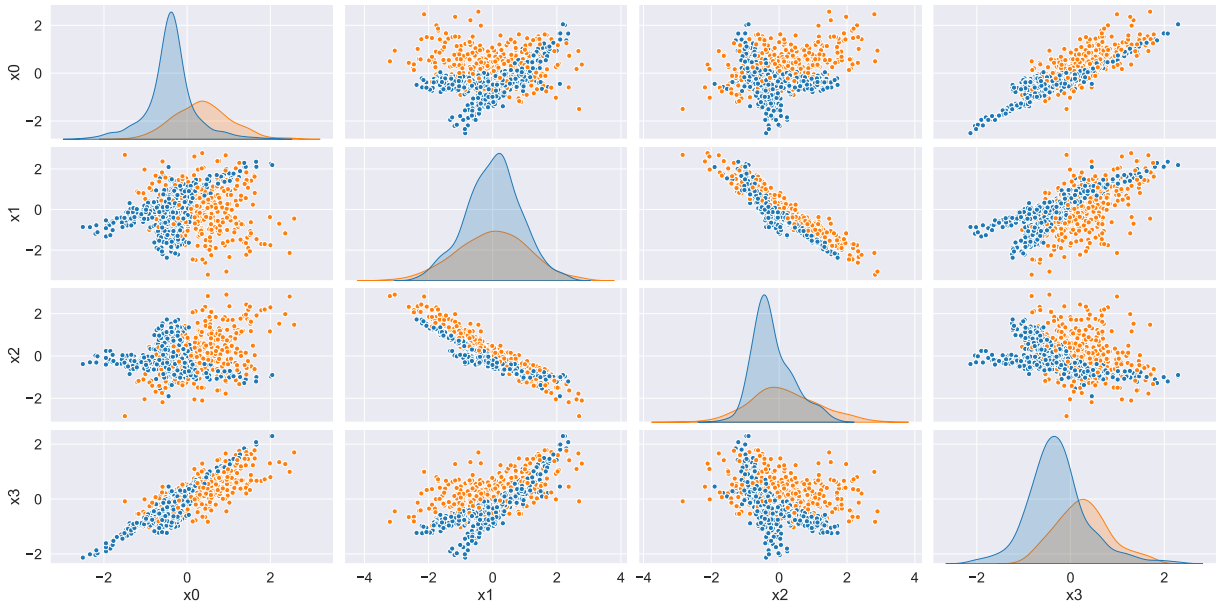


Figure 4: Classes distribution and relationship between features for the Synthetic dataset.

performance using classical algorithms. However, the reduced number of samples allows to perform test series with lower computational load.

4.2 Architectures and environment description

The learning architectures used for each of the datasets are detailed below.

First, a C-Support Vector Machine (SVC) is trained to have a classical baseline. Its hyperparameters ($C = 1.0$ and Radial Basis Function kernel) are set by default and have not been optimized, since the objective of this paper is not to achieve better results than the classical approach.

The VQC circuit is defined as $\mathcal{C} = (\mathcal{D}, \mathcal{M}, \mathcal{E}, \mathcal{P})$, following the same structure as defined in the previous sections. This allows the use of BPQCO approach. For the experiments, certain parameters are fixed a priori, so that the focus is solely on the construction of a specific ansatz for each classification problem. The design parameters \mathcal{D} are set to $N_{qubits} = 4$ and $N_{gates} = 5$. The reason for selecting that number of qubits is that both datasets have four features. As for the maximum number of gates per qubit, it has been selected based on some preliminary tests. Additionally, the ZZFeatureMap circuit is chosen as the feature map \mathcal{M} , since the number of features and N_{qubits} are the same. Thus, the circuit to be optimized $\hat{\mathcal{C}}$ depends only on the ansatz design: $\hat{\mathcal{C}} = (\hat{\mathcal{E}}, \hat{\mathcal{P}}|\mathcal{D}, \mathcal{M})$. To highlight the value of the proposed approach, it is worth noting that the number of possible combinations is $7.78 \cdot 10^{25}$, due to the 12 binary variables and 20 categorical variables (with 13 possible values) to be explored.

In addition, the following common ansatz templates are used to compare performance and establish a quantum baseline:

- **RealAmplitudes:** This circuit template is composed of alternating layers of Y-rotations and CX gate entanglements used as a classification circuit in QML. The prepared quantum states have real amplitudes (the complex part is always zero).
- **EfficientSU2:** The architecture of this circuit is composed of layers of single qubit operations spanned by SU(2) and CX entanglements. This heuristic pattern serves as a tool to prepare trial wave functions for VQAs or to construct VQCs for QML. SU(2) refers to Special Unitary group of degree 2, using 2×2 unitary matrices with determinant 1, like the Pauli rotation gates.
- **PauliTwoDesign:** Comprising alternating rotation and entanglement layers, the circuit begins with an initial layer of $\sqrt{H} = RY(\pi/4)$ gates. The rotation layers feature single-qubit Pauli rotations, randomly selecting axes from X, Y, or Z. The entanglement layers consist of pairwise CZ gates with depth of 2. It is a particular form of a two-design circuit [Nakata et al., 2017], which is frequently studied in QML.

PauliTwoDesign circuit has its own entanglement scheme, while the other two have different type of entanglement implemented: linear, reverse lineal (full) and circular entanglement. Additionally, all of them are tested with different repetition numbers (ranging from 1 to 5) to evaluate their performance across various circuit depths. Obviously, to establish the baseline, the best performing configuration is selected.

In this case, all VQCs, both the templates and the circuits obtained using the BPQCO approach, are simulated in an ideal quantum environment (the reader is advised that noise will be included in the next section of the paper) using the IBM Qiskit library². This includes the absence of noise and decoherence errors, as well as full connection between all qubits. For that purpose, the Sampler³ used to simulate the performance of an ideal quantum computer has a noiseless backend constructed with the density matrix method and 1024 shots.

Finally, the COBYLA (Constrained Optimization BY Linear Approximation) optimizer [Powell, 1994] is selected to train each of the VQCs, as it is a non-gradient based optimization method that significantly speeds up the learning process. The maximum number of evaluations of the function is set to 100.

4.3 Results and discussion

To obtain results, the K -Fold method is used with $K = 10$ and a ratio of 0.7/0.3 for training/validation subsets. In this way, each VQC is independently trained 10 times, and the average accuracy in the validation subsets is obtained as a metric for performance comparison.

First, the SVC is implemented for each of the datasets, obtaining an accuracy of 0.8263 ± 0.0142 for the synthetic dataset and 0.9533 ± 0.0271 for the Iris dataset. As mentioned above, the SVC hyperparameters are not optimized.

²The versions used for testing are as follows: qiskit: 0.44.1, qiskit-aer: 0.12.2, qiskit-algorithms: 0.2.1, qiskit-machine-learning: 0.6.1, and qiskit-terra: 0.25.1.

³The Sampler is an IBM Qiskit service that computes the quasi-probabilistic distribution of bitstrings from quantum circuits.

Table 1: Configuration of each type of circuit template to set the baseline for each dataset. Note that `PauliTwoDesign` has a predefined entanglement scheme.

dataset	RealAmplitudes		EfficientSU2		PauliTwoDesign
	reps.	entanglement	reps.	entanglement	reps.
Synthetic	4	Full	5	Full	2
Iris	2	Linear	3	Full	3

Table 2: Results obtained using the different ansatze for each dataset in terms of accuracy. The subscript i indicates that the quantum simulation environment is under ideal conditions.

Ansatz	Dataset	
	Synthetic	Iris
RealAmplitudes _{i}	0.7448 ± 0.0407	0.7667 ± 0.0559
EfficientSU2 _{i}	0.7465 ± 0.0348	0.7729 ± 0.0657
PauliTwoDesign _{i}	0.6507 ± 0.0550	0.7400 ± 0.0770
BPQCO _{i}	0.8124 ± 0.0231	0.9133 ± 0.0393

However, this allows us to establish a benchmark from a classical point of view, although the goal of this paper is not to outperform them.

The next step is to establish a quantum baseline using the circuit templates described above, and to obtain the best entanglement scheme and number of repetitions for each of them. This is done by running all possible configurations to get the best possible performance and to establish a true baseline. The best configurations obtained for each type of circuit are shown in the Table 1.

Finally, the BPQCO approach is performed to obtain the most suitable circuits for each of the datasets. For this purpose, 600 and 700 trials are run for the Synthetic and Iris datasets, respectively. After that, the best ansatze are obtained, which are shown in Figure 7.

Table 2 presents the results obtained with the different circuits. It shows the average accuracy and its standard deviation in the K-Fold validation subsets with 5 different initializations of the Sampler of the quantum environment (under ideal conditions). These initializations are done in order to study also the stability of the solutions. As can be seen, the results obtained with BPQCO circuits significantly outperform those of typical template circuits. In addition, BPQCO’s results show increased stability of its solutions. Therefore, it can be concluded that it is important to adapt the circuit for each problem. However, in the next section we go a step further to analyze the behavior of these circuits under noisy conditions.

5 A first step towards real quantum environments

Up to this point, the paper has presented a process for finding suitable circuits for a given problem. However, this has been done from an ideal point of view without considering noise, decoherence errors, or the coupling map among qubits. Therefore, it is expected that the performance of the previously obtained circuits will not be as good when implemented on real quantum hardware. Thus, this behavior is analyzed in this section and two alternatives are proposed to adapt the circuits to existing quantum environments.

5.1 Noisy environment simulation

First, a simulation environment is chosen that takes into account the real characteristics of a quantum computer. The reason for opting for simulation is the time associated with execution on real quantum hardware (waiting queues or the connection interface between the execution environment, the platform, and the hardware). In order to obtain reliable results, each circuit has to be executed several times. In addition, it has been found that the BPQCO method requires the execution of hundreds of trials to improve the results. For both reasons, execution on real hardware would not allow exhaustive testing due to the time required. For this purpose, IBM’s `FakeBackend` is chosen. The fake backends are designed to replicate the actions of IBM Quantum systems by using system snapshots. These snapshots contain key information about the quantum system, such as the coupling map, basis gates, qubit properties (as the error rate), which are useful for testing the transpiler and running noisy simulations of the system. It is important to note the significance



Figure 5: Coupling map (qubit interconnection) of the FakeManila backend.

of the transpiled circuit, since it is composed only of those gates supported by the specific quantum computer being used, also considering the coupling map. This is due to the fact that gates involving multiple qubits may need intermediate SWAP gates to match the coupling map. In this case, FakeManila is chosen, a 5-qubit backend that simulates the real operation of IBM’s Manila quantum computer. Figure 5 shows the coupling map of the selected backend, in which the actual connection between the different qubits can be observed. On the other hand, the basis gates supported by this environment are the following: ID, RZ, SX, X, CX, and RESET. Therefore, all circuits executed in such environment must be transpiled to use only these gates.

Once the environment is prepared, the circuits obtained by BPQCO_i (under ideal conditions) are executed in this noisy environment. The Synthetic dataset shows a significant decrease in performance, with an accuracy of 0.7027 ± 0.0589 , representing a 10.97% degradation. Similarly, the Iris dataset also experiences a considerable degradation (48.75%), with an accuracy of 0.4258 ± 0.0664 in the noisy environment. The baseline circuits also suffer degradation, with a 5.52% and 8.05% decrease in performance for the Synthetic and Iris datasets, respectively. These results were expected and, in fact, reinforce the need to adapt the procedure presented above to the noisy environment. Thus, two potential alternatives are presented below.

5.2 Circuit optimization under noise conditions

In order to adapt the designed circuits to both the problem to be solved and the quantum hardware to be used, two design alternatives based on the BPQCO process are presented. The first will be executed directly in the simulated noisy environment, while the second will attempt to incorporate some of the characteristics of the noisy environment into the circuit optimization process.

5.2.1 BPQCO in the noisy environment

The first alternative is to implement the BPQCO approach directly in the simulated noisy environment. This requires transpiling each circuit designed for execution in the environment (in this case, FakeManila backend), taking into account the supported gates and the coupling map. The simulator will also consider the error characteristics of each qubit associated with the noise. Thus, the process is the same, but executed in a noisy environment. The circuit that maximizes the objective function should offer consistent performance when executed in real hardware.

This approach’s execution times are longer than the ideal case due to simulating all the effects of the real environment. However, these run times are still much lower than those associated with direct execution on real hardware. Direct execution on the quantum computer would entail a higher cost of resources (economic and time). Therefore, it is recommended to simulate the circuit optimization based on the problem requirements and available systems before implementation.

5.2.2 Multi-objective BPQCO

As a second option, the possibility of finding a suitable circuit for a specific hardware by altering the optimization process is explored. For this purpose, we propose the use of a multi-objective optimization. In this approach there are now two objective functions: The metric (whose performance is to be maximized) and the circuit complexity (which is to be minimized). For this purpose, the Bayesian TPE algorithm is again used, but adapted to multi-objective search [Ozaki et al., 2022]. The motivation for this new approach is to incorporate real environment information while still working in an ideal environment to reduce execution time.

To do this, it is necessary to define the objective function related to the complexity of the circuit. For this purpose, the transpiled circuit $\mathcal{C}_{\mathcal{T}}$ is used, considering the supported basis gates and the coupling map, which implies an adaptation of the circuit C . This leads to a larger number of basis gates. Once $\mathcal{C}_{\mathcal{T}}$ is known, its complexity is computed by summing the error associated with each of its basis gates in each qubit, values that are available in the backend properties.

Table 3: Complexity of each of the circuits obtained by the different BPQCO variants.

Ansatz	Dataset	
	Synthetic	Iris
BPQCO _i	0.5693	0.4886
BPQCO _n	0.3695	0.3385
Multi-objective BPCQCO	0.1854	0.2205

Therefore, by means of the multi-objective search, the aim is to obtain the transpiled circuit with the lowest possible complexity (to be less susceptible to errors) that obtains the best results.

5.3 Results under noise conditions and discussion

To complete the experimental tests, the two design alternatives described above are used for the same datasets (Synthetic and Iris). Again, FakeManila backend is used to simulate the real environment. In addition, all tests are carried out using the same criteria as above to allow a proper comparison: 10-Fold with the same splits between train/test in each fold and averaging of the accuracy in 5 different runs by changing the backend initialization seeds.

First, a preliminary search for the best predefined circuit to set a noisy baseline performance, denoted as baseline_n, is performed. In both datasets, the best performance with a predefined circuit is obtained with the EfficientSU2 circuit. In the case of the synthetic dataset, with circular entanglement and 1 repetition. For the Iris, with reverse linear entanglement and 3 repetitions.

Then, the first variant of BPQCO (subsection 5.2.1) approach is applied in the noisy environment, denoted as BPQCO_n. For this purpose, 400 and 500 trials are run for the Synthetic and Iris datasets, respectively. After that, the circuits represented in Figure 7 are obtained as those with the best performance in the noisy environment. When compared with those obtained previously, it can be seen that the number of gates decreases in both datasets. It is worth noting the decrease in the use of controlled gates. In the Synthetic dataset, there has been a decrease from 23 controlled gates in the ideal environment to 18 in the noisy environment. As for the Iris dataset, the number of controlled gates has been reduced from 21 to 16. It has specially decreased the number of controlled rotations on the X axis, from 9 to 4. While the number of controlled rotations on the Z axis has increased from 3 to 7. In both cases, the number of CNOT gates used to add entanglement has also decreased.

Finally, the multi-objective BPQCO (5.2.2) is applied, running the same number of trials as in the previous case for each dataset. It is reminded that this approach performs the optimization (design) of the circuit in the ideal environment with the objective of being subsequently executed in the noisy environment. In this case, there is no “best” circuit, but a set of efficient solutions, defined by a Pareto Front, is obtained. Therefore, this set of circuits is evaluated and the one with the best performance in terms of average accuracy and stability is selected. After that, the circuits shown in Figure 7 are selected. Analyzing the obtained circuits, it is evident that they are much simpler, greatly reducing the number of gates used. Again, the major reduction in both cases is in the number of controlled gates, especially the CNOTs for entanglement. Table 3 shows the value of the complexity function associated with each circuit. Evidently, the lowest complexity is that of the multi-objective approach, since in this approach the aim was to minimize this aspect while maximizing performance.

The results on average (10-fold with 5 seed initialization of each backend) of the whole complete process are presented in Figure 6. In it, the potential of BPQCO in both the ideal and noisy environment can be observed. In addition, in order to complete the statistical study of the results, Cohen’s coefficient d_C is used to quantify the effect size. It is considered that if the value is greater than 0.5 the effect is medium and if it is bigger than 0.8 the effect is large [Sawilowsky, 2009]. Therefore, it can be concluded that the effect is large in the ideal environment and medium-large in the noisy environment.

6 Conclusions and further work

Throughout this article, the importance of designing specific PQCs to solve a problem has been demonstrated. Of course, there are agnostic circuit templates that can provide good performance. However, this process of adapting the circuit involves a significant increase in the performance of the solution. For this purpose, we decided to use Bayesian optimization for circuit design, but other search strategies can be equally effective. To this end, we have presented different design aspects and a nomenclature/formulation with the aim of standardizing the parameters to be explored

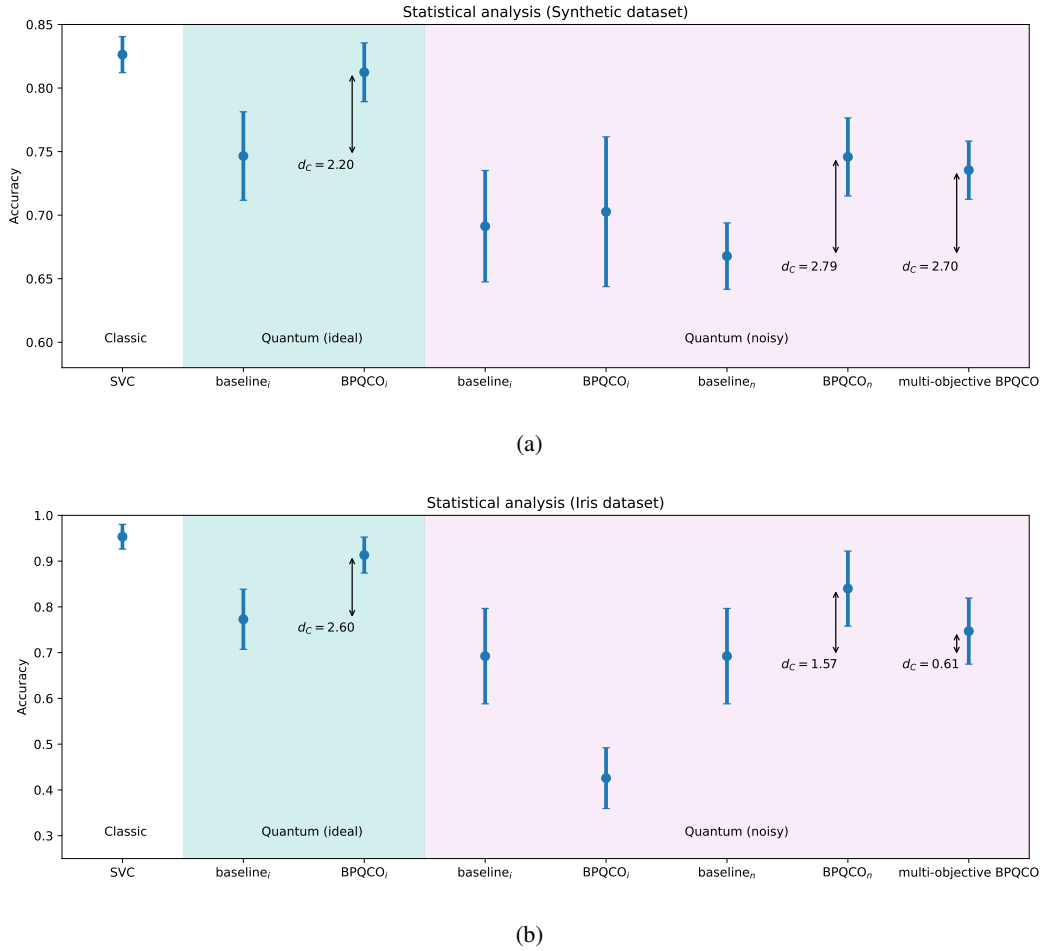


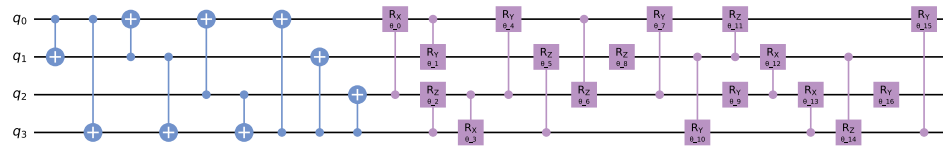
Figure 6: Average Accuracy and standard deviation obtained for each design for the (a) Synthetic and (b) Iris datasets. The subscript indicates under which conditions (i for ideal and n for noisy) the circuit has been designed. The background shows in which environment each design has been run: white for the classical SVC, green for the ideal quantum environment and violet for the noisy quantum environment. Cohen's coefficient d_C is calculated for each design obtained by BPQCO and its variants with respect to the baseline of each case (ideal or noisy).

during the search. After extensive testing (analyzing not only performance but also stability), the BPQCO process has significantly improved the results obtained by predefined circuits.

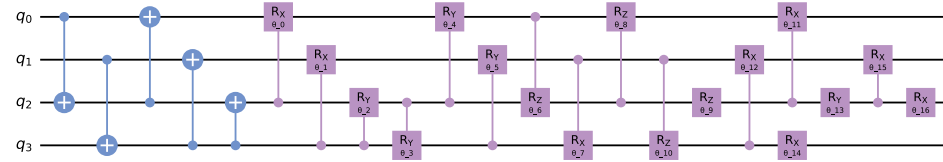
Nonetheless, the most outstanding contribution of this work is the additional step taken to evaluate these circuits in real hardware conditions. This has shown the significant degradation that results presented in an ideal environment can suffer in today's noisy environments. To this end, two alternatives have been proposed, focusing on the adaptation of the circuit to the hardware. Again, the results obtained have met the expectations and objectives set, since they significantly improve the performance, resulting in circuits with less complexity and, therefore, less vulnerable to the effects of noise.

On the other hand, in order to simplify the experiments, the PQC design has focused on the search for the best ansatz. However, other aspects can be included in the search process, such as the number of qubits, the depth of the system, or the data encoding method, in which data re-uploading can be explored. In addition, the gates to be used can be modified by those supported by photonic computers for the use of continuous variable [Killoran et al., 2019].

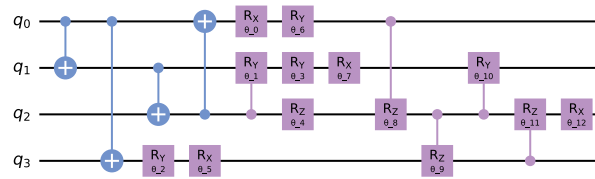
Finally, it is worth mentioning that we intend to incorporate the BPQCO process to other open lines. The goal is to adapt PQCs used for solving other more complex problems in the field of Earth Observation in which we are currently involved. This includes the design of hybrid models that incorporate VQCs in their architecture, as well as the design of VQEs for optimization tasks [Makarov et al., 2024].



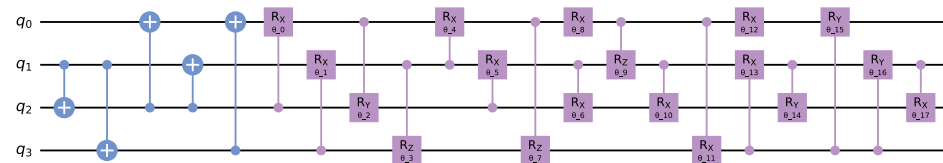
(1.a)



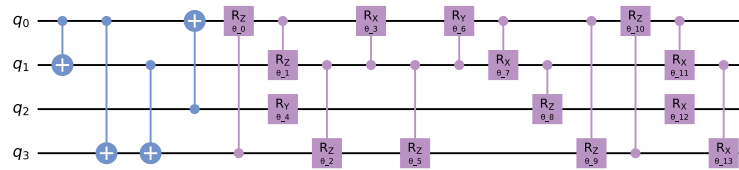
(1.b)



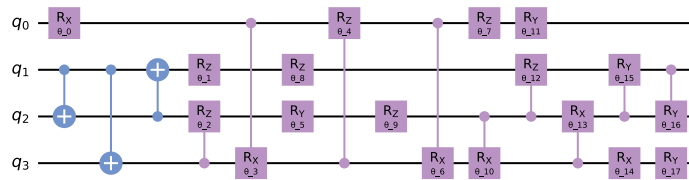
(1.c)



(2.a)



(2.b)



(2.c)

Figure 7: Best BPQCO circuits in the (a) ideal environment, (b) noisy environment and (c) multi-objective method for the (1) Synthetic and (2) Iris datasets.

Acknowledgments

This work has been supported by the Spanish Ministry of Science and Innovation under the Recovery, Transformation and Resilience Plan (Misiones CUCO Grant MIG-20211005).

References

- Christopher M Bishop and Hugh Bishop. The deep learning revolution. In *Deep Learning: Foundations and Concepts*, pages 1–22. Springer, 2023. doi:https://doi.org/10.1007/978-3-031-45468-4_1.
- Jacob Biamonte, Peter Wittek, Nicola Pancotti, Patrick Rebentrost, Nathan Wiebe, and Seth Lloyd. Quantum machine learning. *Nature*, 549(7671):195–202, 2017. doi:<https://doi.org/10.1038/nature23474>.
- Ilya Sinayskiy Maria Schuld and Francesco Petruccione. An introduction to quantum machine learning. *Contemporary Physics*, 56(2):172–185, 2015. doi:10.1080/00107514.2014.964942.
- Michael A Nielsen and Isaac L Chuang. *Quantum computation and quantum information*. Cambridge University Press, 2010.
- John Preskill. Quantum Computing in the NISQ era and beyond. *Quantum*, 2:79, aug 2018. ISSN 2521-327X. doi:10.22331/q-2018-08-06-79.
- Kamila Zaman, Alberto Marchisio, Muhammad Abdullah Hanif, and Muhammad Shafique. A survey on quantum machine learning: Current trends, challenges, opportunities, and the road ahead. *arXiv preprint arXiv:2310.10315*, 2023. doi:<https://doi.org/10.48550/arXiv.2310.10315>.
- Elias F. Combarro, Samuel González-Castillo, and Alberto Di Meglio. *A Practical Guide to Quantum Machine Learning and Quantum Optimization: Hands-on Approach to Modern Quantum Algorithms*. Packt Publishing Ltd, 2023.
- Patrick Rebentrost, Masoud Mohseni, and Seth Lloyd. Quantum support vector machine for big data classification. *Phys. Rev. Lett.*, 113:130503, Sep 2014. doi:10.1103/PhysRevLett.113.130503.
- Maxwell Henderson, Samridhi Shakya, Shashindra Pradhan, and Tristan Cook. Quconvolutional neural networks: powering image recognition with quantum circuits. *Quantum Machine Intelligence*, 2(1):2, 2020. doi:<https://doi.org/10.1007/s42484-020-00012-y>.
- Seunghyeok Oh, Jaeho Choi, and Joongheon Kim. A tutorial on quantum convolutional neural networks (qcnn). In *2020 International Conference on Information and Communication Technology Convergence (ICTC)*, pages 236–239, 2020. doi:10.1109/ICTC49870.2020.9289439.
- Yuto Takaki, Kosuke Mitarai, Makoto Negoro, Keisuke Fujii, and Masahiro Kitagawa. Learning temporal data with a variational quantum recurrent neural network. *Phys. Rev. A*, 103:052414, May 2021. doi:10.1103/PhysRevA.103.052414.
- Sukin Sim, Peter D Johnson, and Alán Aspuru-Guzik. Expressibility and entangling capability of parameterized quantum circuits for hybrid quantum-classical algorithms. *Advanced Quantum Technologies*, 2(12):1900070, 2019. doi:<https://doi.org/10.1002/qute.201900070>.
- Suguru Endo, Zhenyu Cai, Simon C. Benjamin, and Xiao Yuan. Hybrid quantum-classical algorithms and quantum error mitigation. *Journal of the Physical Society of Japan*, 90(3):032001, 2021. doi:10.7566/JPSJ.90.032001.
- Marcello Benedetti, Erika Lloyd, Stefan Sack, and Mattia Fiorentini. Parameterized quantum circuits as machine learning models. *Quantum Science and Technology*, 4(4):043001, nov 2019. doi:10.1088/2058-9565/ab4eb5.
- Alona Sakhnenko, Corey O’Meara, Kumar JB Ghosh, Christian B Mendl, Giorgio Cortiana, and Juan Bernabé-Moreno. Hybrid classical-quantum autoencoder for anomaly detection. *Quantum Machine Intelligence*, 4(2):27, 2022. doi:<https://doi.org/10.1007/s42484-022-00075-z>.
- Samuel Yen-Chi Chen, Shinjae Yoo, and Yao-Lung L. Fang. Quantum long short-term memory. In *ICASSP 2022 - 2022 IEEE International Conference on Acoustics, Speech and Signal Processing (ICASSP)*, pages 8622–8626, 2022. doi:10.1109/ICASSP43922.2022.9747369.
- Danyal Maheshwari, Daniel Sierra-Sosa, and Begonya Garcia-Zapirain. Variational quantum classifier for binary classification: Real vs synthetic dataset. *IEEE Access*, 10:3705–3715, 2022. doi:10.1109/ACCESS.2021.3139323.
- Asel Saginalieva, Mo Kordzanganeh, Andrii Kurkin, Artem Melnikov, Daniil Kuhmistrov, Michael Perelshtein, Alexey Melnikov, Andrea Skolik, and David Von Dollen. Hybrid quantum resnet for car classification and its hyperparameter optimization. *Quantum Machine Intelligence*, 5(2):38, 2023. doi:<https://doi.org/10.1007/s42484-023-00123-2>.

- Hao-Yuan Chen, Yen-Jui Chang, Shih-Wei Liao, and Ching-Ray Chang. Deep q-learning with hybrid quantum neural network on solving maze problems. *Quantum Machine Intelligence*, 6(1):2, 2024. doi:<https://doi.org/10.1007/s42484-023-00137-w>.
- Yoshifumi Nakata, Christoph Hirche, Ciara Morgan, and Andreas Winter. Unitary 2-designs from random X- and Z-diagonal unitaries. *Journal of Mathematical Physics*, 58(5):052203, 05 2017. ISSN 0022-2488. doi:10.1063/1.4983266.
- Thomas Hubregtsen, Josef Pichlmeier, Patrick Stecher, and Koen Bertels. Evaluation of parameterized quantum circuits: on the relation between classification accuracy, expressibility, and entangling capability. *Quantum Machine Intelligence*, 3:1–19, 2021. doi:<https://doi.org/10.1007/s42484-021-00038-w>.
- Sebastian Raubitzek and Kevin Mallinger. On the applicability of quantum machine learning. *Entropy*, 25(7), 2023. ISSN 1099-4300. doi:10.3390/e25070992.
- Sergio Altares-López, Juan José García-Ripoll, and Angela Ribeiro. Autoqml: Automatic generation and training of robust quantum-inspired classifiers by using evolutionary algorithms on grayscale images. *Expert Systems with Applications*, 244:122984, 2024. ISSN 0957-4174. doi:<https://doi.org/10.1016/j.eswa.2023.122984>.
- Mohammad Pirhooshyaran and Tamás Terlaky. Quantum circuit design search. *Quantum Machine Intelligence*, 3(2):25, 2021. ISSN 2524-4906, 2524-4914. doi:10.1007/s42484-021-00051-z.
- Yuxuan Du, Tao Huang, Shan You, Min-Hsiu Hsieh, and Dacheng Tao. Quantum circuit architecture search for variational quantum algorithms. *npj Quantum Information*, 8(1):62, 2022. doi:<https://doi.org/10.1038/s41534-022-00570-y>.
- Giuseppe Buonaiuto, Francesco Gargiulo, Giuseppe De Pietro, Massimo Esposito, and Marco Pota. The effects of quantum hardware properties on the performances of variational quantum learning algorithms. *Quantum Machine Intelligence*, 6(1):9, 2024. doi:<https://doi.org/10.1007/s42484-024-00144-5>.
- Maria Schuld and Nathan Killoran. Quantum machine learning in feature hilbert spaces. *Physical Review Letters*, 122(4), feb 2019. doi:10.1103/physrevlett.122.040504.
- Manuela Weigold, Johanna Barzen, Frank Leymann, and Marie Salm. Expanding data encoding patterns for quantum algorithms. In *2021 IEEE 18th International Conference on Software Architecture Companion (ICSA-C)*, pages 95–101, 2021. doi:10.1109/ICSA-C52384.2021.00025.
- Adrián Pérez-Salinas, Alba Cervera-Lierta, Elies Gil-Fuster, and José I. Latorre. Data re-uploading for a universal quantum classifier. *Quantum*, 4:226, February 2020. ISSN 2521-327X. doi:10.22331/q-2020-02-06-226.
- Toshiaki Koike-Akino, Pu Wang, and Ye Wang. Autoqml: Automated quantum machine learning for wi-fi integrated sensing and communications. In *2022 IEEE 12th Sensor Array and Multichannel Signal Processing Workshop (SAM)*, pages 360–364, 2022. doi:10.1109/SAM53842.2022.9827846.
- James Bergstra, Rémi Bardenet, Yoshua Bengio, and Balázs Kégl. Algorithms for hyper-parameter optimization. In J. Shawe-Taylor, R. Zemel, P. Bartlett, F. Pereira, and K.Q. Weinberger, editors, *Advances in Neural Information Processing Systems*, volume 24. Curran Associates, Inc., 2011. URL https://proceedings.neurips.cc/paper_files/paper/2011/file/86e8f7ab32cf12577bc2619bc635690-Paper.pdf.
- R. A. Fisher. Iris. UCI Machine Learning Repository, 1988. URL <https://doi.org/10.24432/C56C76>.
- M. J. D. Powell. *A Direct Search Optimization Method That Models the Objective and Constraint Functions by Linear Interpolation*, pages 51–67. Springer Netherlands, Dordrecht, 1994. ISBN 978-94-015-8330-5. doi:10.1007/978-94-015-8330-5_4.
- Yoshihiko Ozaki, Yuki Tanigaki, Shuhei Watanabe, Masahiro Nomura, and Masaki Onishi. Multiobjective tree-structured parzen estimator. *Journal of Artificial Intelligence Research*, 73:1209–1250, 2022. doi:<https://doi.org/10.1613/jair.1.13188>.
- Shlomo S Sawilowsky. New effect size rules of thumb. *Journal of modern applied statistical methods*, 8(2):26, 2009. doi:<https://doi.org/10.22237/jmasm/1257035100>.
- Nathan Killoran, Thomas R. Bromley, Juan Miguel Arrazola, Maria Schuld, Nicolás Quesada, and Seth Lloyd. Continuous-variable quantum neural networks. *Phys. Rev. Res.*, 1:033063, Oct 2019. doi:10.1103/PhysRevResearch.1.033063.
- Antón Makarov, Carlos Pérez-Herradón, Giacomo Franceschetto, Márcio M. Taddei, Eneko Osaba, Paloma del Barrio, Esther Villar-Rodríguez, and Izaskun Oregi. Quantum optimization methods for satellite mission planning. *arXiv preprint arXiv:2404.05516 [quant-ph]*, 2024. doi:<https://doi.org/10.48550/arXiv.2404.05516>.